Signature: © Pol J Radiol, 2017; 82: 345-355
DOI: 10.12659/PJR.900633

Polish Journal of Radiology
www.PolRadiol.com
ORIGINAL ARTICLE

Received: 2016.07.16
Accepted: 2016.09.27
Published: 2017.06.28

Can Diffusion Weighted Imaging Aid in Differentiating Benign from Malignant Sinonasal Masses?: A Useful Adjunct

Authors' Contribution:
A Study Design
B Data Collection
C Statistical Analysis
D Data Interpretation
E Manuscript Preparation
F Literature Search
G Funds Collection

Abanti Das[1ABDEF], Ashu S. Bhalla[1ACDE], Raju Sharma[1ACDE], Atin Kumar[1ABF], Alok Thakar[2ABCF], Vishnubhatla Sreenivas M.[3ABCD], Mehar C. Sharma[4ABE], Suresh C. Sharma[2AEF]

[1] Department of Radiodiagnosis, All India Institute of Medical Sciences, New Delhi, India
[2] Department of Otolaryngorhinology, All India Institute of Medical Sciences, New Delhi, India
[3] Department of Biostatistics, All India Institute of Medical Sciences, New Delhi, India
[4] Department of Pathology, All India Institute of Medical Sciences, New Delhi, India

Author's address: Ashu Seith Bhalla, Department of Radiodiagnosis, All India Institute of Medical Sciences, Ansari Nagar, New Delhi-110029, India, e-mail: ashubhalla1@yahoo.com

Summary

Background: To evaluate the role of diffusion weighted imaging (DWI) and apparent diffusion coefficient (ADC) values at 3 Tesla in characterizing sinonasal masses.

Material/Methods: After ethical clearance, 79 treatment naive patients with head and neck masses underwent magnetic resonance imaging (MRI), including DWI at 3 Tesla using the following b values – 0, 500 and 1000 s/mm^2. Thirty-one patients were found to have sinonasal tumours and were subsequently analysed. Image analysis consisted of a morphological evaluation of conventional MR images, qualitative evaluation of DW trace images and quantitative assessment of mean ADC values. Receiver operating characteristic (ROC) curve was drawn to determine a cut-off ADC value for the differentiation between benign and malignant masses.

Results: Sinonasal masses showed an overlapping growth pattern on conventional imaging, irrespective of their biological nature. The mean ADC value of benign lesions was $1.948\pm0.459\times10^{-3}$ mm^2/s, while that of malignant lesions was $1.046\pm0.711\times10^{-3}$ mm^2/s, and the difference was statistically significant (p=0.004). When a cut-off ADC value of 1.791×10^{-3} mm^2/s was used, sensitivity of 80% and specificity of 83.3% were obtained for characterization of malignant lesions, which was statistically significant. Juvenile nasopharyngeal angiofibroma (JNA) showed distinctly high ADC values, while meningioma was the only benign lesion with restricted diffusion. Atypical entities with unexpected diffusion characteristics included: adenocarcinoma, adenoid cystic carcinoma, meningioma, chondrosarcoma and fibromyxoid sarcoma.

Conclusions: DWI in conjunction with conventional imaging can potentially enhance the diagnostic accuracy in characterizing sinonasal masses as benign or malignant. Some specific entities such as JNA and meningioma showed distinctive diffusion characteristics.

MeSH Keywords: Diffusion Magnetic Resonance Imaging • Magnetic Resonance Imaging • Paranasal Sinus Neoplasms

PDF file: http://www.polradiol.com/abstract/index/idArt/900633

Background

Sinonasal masses are rare, comprising only 3% of all malignant head and neck tumours [1]. Their clinical presentation is often non-specific, mimicking the more common chronic inflammatory processes. Involvement of adjacent structures leading to facial deformity or functional deficit is usually late, thereby posing a diagnostic challenge to

the treating physician. Certain clinical features, including recurrent symptoms unresponsive to medical therapy or unilateral involvement, are considered suspicious for malignancy which should initiate a more careful search for a definitive diagnosis. This, coupled with the complex anatomy of the region which is not always amenable to adequate clinical evaluation, makes imaging an indispensable part of the workup in patients presenting with a sinonasal pathology.

The most important role of imaging is to show the entire extent of the lesion, including its extension to critical areas of the head and neck, which will dictate the modality of treatment suitable for the patient. Imaging is also expected to differentiate inflammatory from neoplastic aetiologies and further characterize the latter as benign or malignant. But more often than not, arriving at an accurate preoperative diagnosis is not possible due to their overlapping appearances.

Among the existing imaging modalities, computed tomography (CT) is used most commonly for imaging of the head and neck. Magnetic resonance imaging (MRI) is mostly used as a problem solving tool. Diffusion weighted imaging (DWI) is a relatively newer adjunct to MRI and has been used by various investigators to evaluate neck masses and the biological nature of lesions. While most of the earlier studies were conducted at1.5 Tesla (T) field strength, only few recent studies have explored 3T imaging in this anatomic region. Higher field strength with a dedicated 16-channel neurovascular coil can improve the signal-to-noise ratio, thereby producing better quality DWI and apparent diffusion coefficient (ADC) maps compared to 1.5T.

In this study, we used DWI and ADC values acquired on a 3T scanner to see whether differentiation between benign and malignant sinonasal lesions is possible with this functional imaging technique and also whether individual entities can be further characterized.

Material and Methods

Patient details

This ethically approved study was conducted to investigate the role of DWI in characterization of neck masses at 3T over a period from July 2011 to April 2013. Since this work is a sub-part of a larger study involving head and neck masses, our inclusion criteria consisted of adult patients (≥18 years) found to have a neck mass either on clinical examination or on any imaging modality. Patients with prior history of chemo- or radiotherapy were excluded from the study. A total of 79 treatment naive patients were recruited after obtaining informed consent, of whom 31 patients were found to have sinonasal tumours. This study pertains to the 31 patients with sinonasal masses, all of whom underwent MRI, including DWI. Conventional MRI, DW images and ADC maps were prospectively reviewed to study the diffusion characteristics of the lesions. Endoscopic biopsy or operative specimen were obtained in all patients, which served as the gold standard for final diagnosis.

MR image acquisition

All MR scans were performed on a 3T scanner (Achieva 3.0T TX Phillips, Netherlands) using a dedicated 16-channel neurovascular coil. Conventional MRI included axial T1W (TR/TE: 600–700/10–20 msec), axial T2W (TR/TE: 3000–4000/70–90 msec) and coronal T2 fat-saturated (T2FS) images. Additional sequences were used where considered necessary.

Diffusion weighted images were obtained in the axial plane using fat-suppressed, single-shot, spin-echo, echo-planar technique (echo planar imaging factor: 67) with b values of 0, 500 and 1000 s/mm^2. Diffusion probing gradients were applied in all three orthogonal axes to obtain isotropic DW images. The following imaging parameters were used: TR/TE 3400/86 ms, bandwidth: 2588.6 Hz per pixel, matrix size: 152×121, section thickness: 4 mm with 0.4 mm intersection gap, field of view: 230–300 mm, flip angle: 90 degree, number of signal averages: 2, sensitivity encoding factor (SENSE factor): 2. The resultant acquisition time varied from 2 to 3 minutes. Corresponding ADC maps were generated automatically on a commercial workstation.

Image analysis

Image analysis included: (1) morphological evaluation of conventional MR images, (2) qualitative evaluation of DW trace images and (3) quantitative representative ADC values of the lesions.

Morphological evaluation focused on the pattern of lesion growth (expansile/destructive), signal intensity on T1- and T2-weighted images, extension to adjacent areas (intracranial or intra-orbital) and overall appearance (homogeneous/heterogeneous). Conventional MR images were evaluated by 3 radiologists (RS, ASB and AK having 20, 15 and 11 years of experience in MRI, respectively) who were blinded to the final diagnosis, and findings were recorded by consensus.

DW images at b values of 0, 500 and 1000 s/mm^2 were evaluated qualitatively to determine if the lesion showed facilitated or restricted diffusion. If the lesion retained its signal intensity or showed minimal decrease with increasing b values, it was labelled as restricted diffusion, while a drop in signal intensity on increasing b values was regarded as facilitated diffusion. Corresponding ADC maps showed hypointense signal in lesions with restricted diffusion and hyperintense signal in those with facilitated diffusion.

For quantitative evaluation, regions of interest (ROIs) were drawn on the lesions to obtain the representative ADC values. Circular ROIs were placed manually on the lesion on ADC maps using conventional MR images as references to avoid areas of signal inhomogeneity or distortion due to susceptibility artefacts at air-soft tissue interfaces. For lesions which showed significant heterogeneous areas on conventional images, separate ROI measurements were obtained and recorded from those areas. A mean of three such values gave the mean ADC value for the lesion. All ROI measurements were done by a single radiologist who was also blinded to the final diagnosis.

Table 1. Conventional MR imaging features of sinonasal masses.

S. No	Entity (n)	Growth pattern		Overall appearance		Extension	
		E	S	Hom	Het	I/C	I/O
1	JNA (7)	7	7	0	7	7	6
2	Lymphoma (3)	3	2	2	1	1	2
3.	Adenocarcinoma (3)	3	3	0	3	2	2
4.	Adenoid cystic carcinoma (2)	2	1	0	2	1	1
5	SNUC (2)	1	2	0	2	1	2
6	Inflammatory nasal polyp (1)	1	0	0	1	0	0
7	Meningioma (1)	1	0	1	1	0	0
8	Plasmacytoma (1)	1	0	1	0	0	1
9	Esthesioneuroblastoma (1)	1	1	0	1	0	1
10	Inverted papilloma (1)	1	0	0	1	0	0
11	Poorly differentiated carcinoma (1)	0	1	0	1	1	1
12	Transitional carcinoma (1)	0	1	0	1	1	1
13	Malignant melanoma (1)	1	0	0	1	0	0
14	Squamous cell carcinoma (1)	1	1	0	1	0	1
15	Chondrosarcoma (1)	1	1	0	1	1	1
16	Low grade fibromyxoid sarcoma (1)	1	1	0	1	1	1

E – expansile; D – destructive; Hom – homogenous; Het – heterogeneous; I/C – intra-cranial extension; I/O – intra-orbital extension; JNA – juvenile nasopharyngeal angiofibroma; SNUC – sinonasal undifferentiated carcinoma.

Table 2. Diffusion characteristics of sinonasal masses.

S. No	Final diagnosis (n/%)	Mean ADC ±SD ($\times 10^{-3}$ mm^2/s)	Range ($\times 10^{-3}$ mm^2/s)
1	Juvenile nasopharyngeal angiofibroma (7/25)	2.169±0.270	1.791–2.543
2	Lymphoma (3/10.7)	0.483±0.079	0.433–0.575
3	Sinonasal adenocarcinoma (3/10.7)	1.381±0.818	0.853–2.324
4	Adenoid cystic carcinoma (2/7.1)	1.607±0.224	1.448–1.776
5	Sinonasal undifferentiated carcinoma (2/7.1)	0.671±0.009	0.664–0.678
6	Squamous cell carcinoma (1/3.6)	0.433	–
7	Inflammatory nasal polyp (1/3.6)	1.846	–
8	Meningioma (1/3.6)	1.044	–
9	Plasmacytoma (1/3.6)	0.521	–
10	Esthesioneuroblastoma (1/3.6)	0.395	–
11	Inverted papilloma (1/3.6)	1.411	–
12	Poorly differentiated carcinoma (1/3.6)	0.991	–
13	Transitional carcinoma (1/3.6)	0.777	–
14	Malignant melanoma (1/3.6)	0.759	–
15	Chondrosarcoma (1/3.6)	2.696	–
16	Low grade fibromyxoid sarcoma(1/3.6)	2.205	–

Table 3. Comparison of DWI and histology in characterization of sinonasal masses.

		Gold standard (histology)		
		Benign	**Malignant**	**Total (DWI)**
DWI	Facilitated	9	5	14
	Restricted	1	13	14
	Total	10	18	28

DWI – Diffusion weighted imaging.

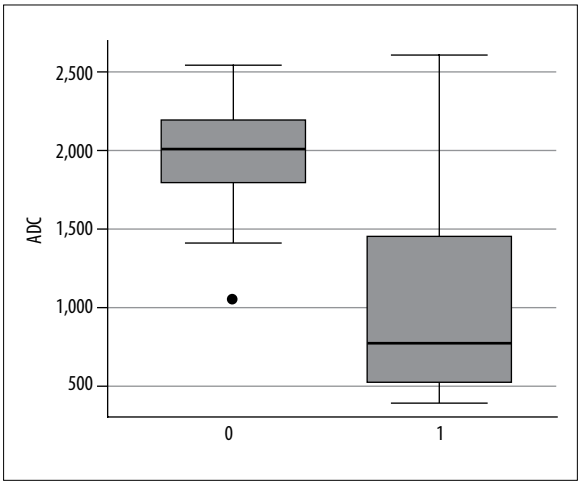

Figure 1. Box and whisker plot showing ADC values in benign and malignant sinonasal masses. 0: benign lesions; 1: malignant lesions.

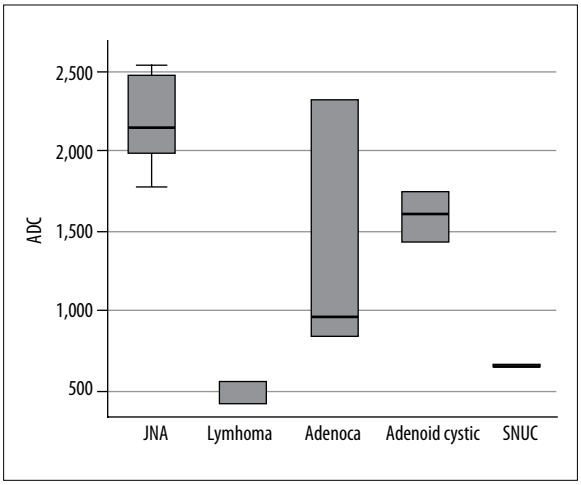

Figure 2. Box and whisker plot of ADC values of common sinonasal masses. JNA – juvenile nasopharyngeal angiofibroma; Adenoca – adenocarcinoma; Adenoid cystic – adenoid cystic carcinoma; SNUC – sinonasal undifferentiated carcinoma.

Statistical analysis was carried out with Stata software, version 12.1. A P value lower than or equal to 0.05 was considered statistically significant.

Results

There were 31 patients with sinonasal masses, of whom three were found to have masses with large areas of haemorrhage on MRI, and hence these patients were excluded from the final analysis since haemorrhage is known to adversely influence the interpretation of DWI.

Of the remaining 28 patients, the majority were males (n=21, 75%) with a mean age of 38.95 years (range: 10 to 66 years). Overall, there were more malignant (n=18, 64.2%) than benign lesions on final histology. All the benign lesions were present in males (n=10, 100%), who also had two-thirds of the malignant lesions (n=12,66.67%).The mean age of patients with malignant lesions was higher (mean: 50.56 years, range: 30 to 70 years) than that of patients with benign lesions (mean: 22.1 years, range: 10 to 52 years), and the difference was statistically significant.

The conventional MR images were analysed to look for predominantly expansile (labelled as E) or predominantly destructive (labelled as D) growth patterns of lesions. In addition, their overall morphology (homogenous or heterogeneous), adjacent extension, i.e. intra-cranial extension (I/C) and intra-orbital extension (I/O), were also assessed.

Table 1 summarizes the imaging appearances of sinonasal masses on conventional MRI.

On DWI, 14 lesions demonstrated facilitated diffusion, while 14 lesions showed restricted diffusion. The final diffusion characteristics and mean ADC values of the lesions are shown in Table 2.

On final histology, 10 lesions were found to be benign and 18 were malignant. Overall results of DWI interpretation, as compared to histology are shown in Table 3.

The ADC values of benign and malignant entities were compared. The mean ADC value of the benign lesions was $1.948 \pm 0.459 \times 10^{-3}$ mm^2/s, while that of malignant lesions was $1.046 \pm 0.711 \times 10^{-3}$ mm^2/s, and the difference was statistically significant (p=0.004, Mann-Whitney U Test), (Figure 1).

We also compared the ADC values of the common entities seen in our series. By using Bonferroni correction of one-way ANOVA test and log ADC values, we found significant differences between the mean ADC value of juvenile nasopharyngeal angiofibroma (JNA) and lymphoma (p=0.000), adenocarcinoma and lymphoma (p=0.046), adenoid cystic carcinoma and lymphoma (p=0.002), (Figure 2).

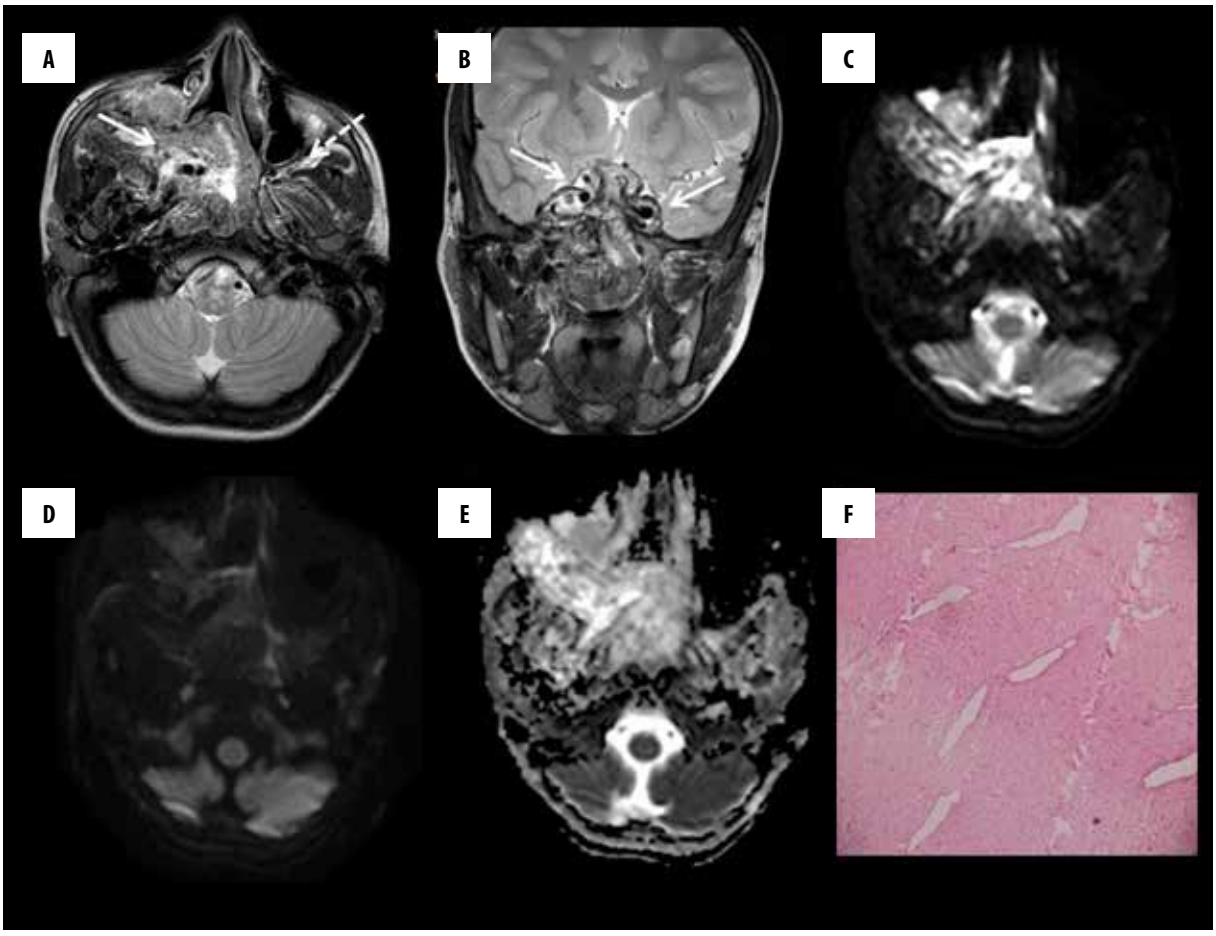

Figure 3. Nasopharyngeal angiofibroma showing facilitated diffusion. (**A**) Axial T2W image shows heterogeneously hyperintense, sinonasal mass with extension to the right infratemporal fossa through the pterygopalatine fossa (solid arrow), (dashed arrow shows normal left pterygopalatine fossa). (**B**) Coronal T2W image shows an intracranial extension encasing intracranial ICA bilaterally (arrows) with prominent vascular flow voids. DW images at b 0 (**C**), b 1000 s/mm^2 (**D**) and ADC map (**E**) show progressive loss of signal on increasing b values suggestive of facilitated diffusion. Mean ADC of lesion: 2.014×10^{-3} mm^2/s. (**F**) Photomicrograph (original magnification, ×100; hematoxylin-eosin [H-E] showing variably sized, thin-walled vessels in a hypocellular fibrous stroma).

Among the benign lesions, the highest mean ADC value was found in JNA (Figure 3), and the lowest in meningioma (Figure 4). Whereas among the malignant lesions, esthesioneuroblastoma had the lowest mean ADC value (Figure 5), and chondrosarcoma showed the highest mean ADC value (not shown).

Overall, the sensitivity, specificity, positive predictive value and negative predictive value of DWI in differentiating between benign and malignant sinonasal masses were: 72.7%, 90%, 92.9%, and 64.3% respectively.

An ROC analysis was done to determine a threshold ADC value for the differentiation between benign and malignant sinonasal masses (Figure 6). A cut-off ADC value of 1.791×10^{-3} mm^2/s yielded a sensitivity of 80%, specificity of 83.3%, with area under the curve (AUC) of 0.83, which was statistically significant for the characterization of malignant lesions.

There were five entities that showed unexpected behaviour on DWI, which was not in concordance with their final histology. These included sinonasal adenocarcinoma (Figure 7), adenoid cystic carcinoma (Figure 8), meningioma (Figure 4) and fibromyxoid sarcoma.

Discussion

Sinonasal masses are uncommon and comprise around 3% of all malignant tumours that occur in the head and neck [1]. A variety of benign and malignant lesions occur in the sinonasal cavity, but malignant lesions tend to be more common [2], and this was also noted in our study (64.3%, n=18).

The most common lesion overall as well as among the benign entities was JNA (25%, n=7), (Figure 3). Among the malignant sinonasal masses, the most common entity was sinonasal lymphoma (10.7%, n=3) and adenocarcinoma (10.7%, n=3). Although the most common malignant neoplasm in the sinonasal cavity is squamous cell carcinoma [3], the unusual prevalence of entities in our series may be explained by two reasons. Firstly, our institution is a tertiary care referral centre for JNAs because of the

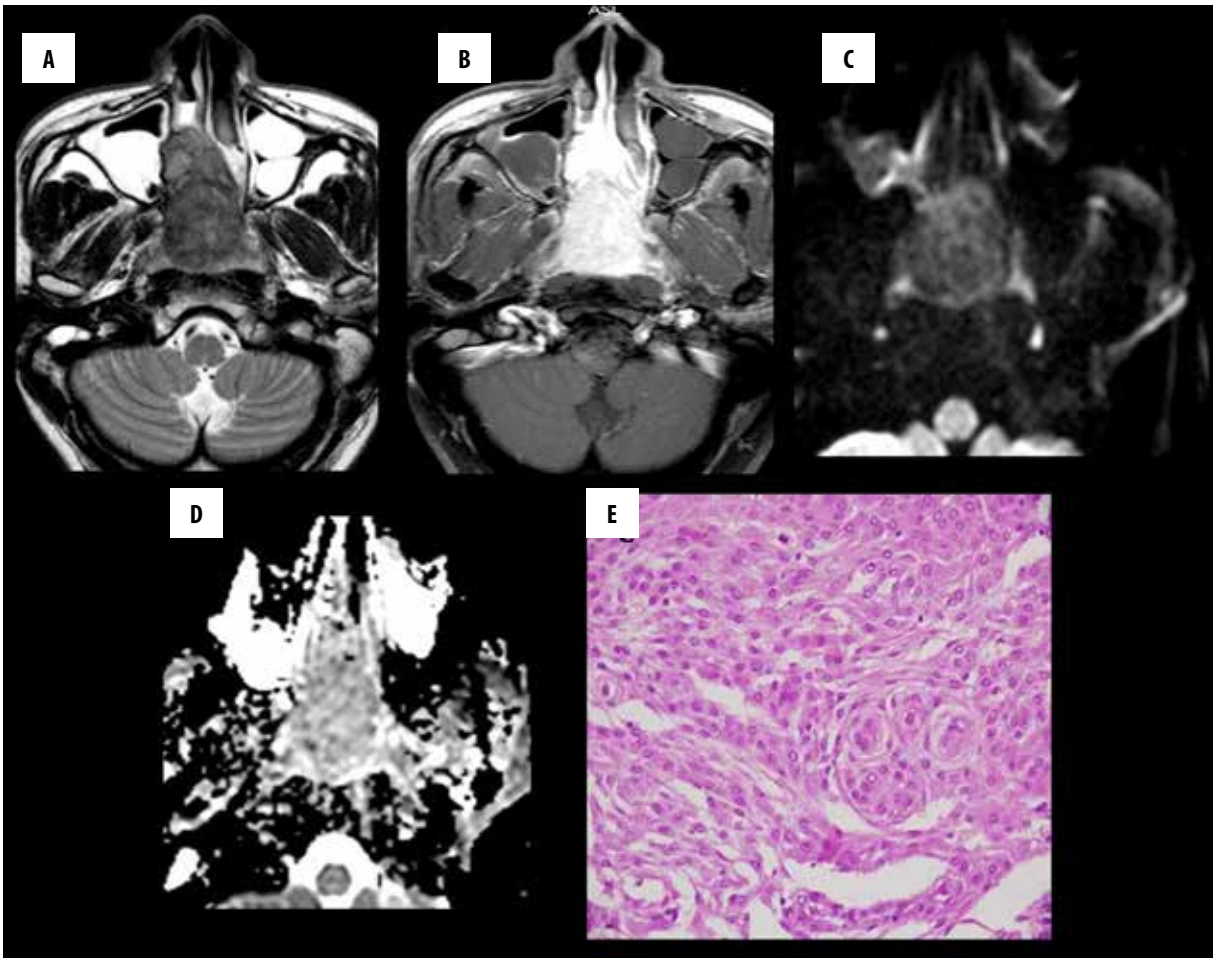

Figure 4. Sinonasal meningioma with restricted diffusion. Axial T2W image (**A**) shows well-defined, mildly expansile iso- to hypointense mass in the nasal cavity and nasopharynx. Axial T1W, fat-saturated, post-gadolinium image (**B**) shows a mass with avid homogenous enhancement. DW image at b 1000 (**C**) s/mm^2 and corresponding ADC map (**D**) reveal restricted diffusion. Mean ADC value: 1.044×10^{-3} mm^2/s. (**E**) Photomicrograph (original magnification, ×400; [H-E]) showing tumour cells arranged in sheets and whorls.

availability of local expertise and hence there is an inherent referral bias. Secondly, this work was done in collaboration with our Otolaryngorhinology department, while most cases of squamous cell carcinoma are referred to the oncology centre in our hospital.

The imaging features of benign and malignant sinonasal masses on conventional CT and MRI frequently overlap and hence accurate differentiation between the two may not always be possible. Traditionally, a pattern approach has been used to narrow down the differential diagnosis of sinonasal masses, although this has not proven to be very specific in predicting the final histology [3]. In our series, there was an overlapping growth pattern of lesions with all the JNAs showing both osseous erosion and remodelling. Among malignant lesions, lymphomas showed predominantly expansile growth pattern, while squamous cell carcinoma showed both patterns. This overlapping growth pattern results in the limitation of conventional imaging in characterizing sinonasal masses as benign or malignant. Hence, there is a need for an additional paradigm to improve characterization, and DWI may be able to fulfil this need.

Few of the studies that have explored the role of DWI in evaluation of sinonasal masses have been compiled in Table 4.

Most of the earlier studies were performed on 1.5T field strength, but whether the values obtained are applicable to higher field strength imaging is not known clearly [9]. In concordance with previous literature, our study also showed a significant difference between the mean ADC values of benign ($1.948\pm0.459\times10^{-3}$ mm^2/s) and malignant lesions ($1.046\pm0.711\times10^{-3}$ mm^2/s, p=0.004), with a threshold ADC value of 1.791×10^{-3} mm^2/s for differentiation between benign and malignant lesions with a sensitivity of 80% and specificity of 83.3%.

In our study, among all the entities, the highest mean ADC value was seen in JNA ($2.168\pm0.270\times10^{-3}$ mm^2/s) (Figure 3). Although we could not find supportive evidence in the literature for this finding, a possible two-fold hypothesis could be proposed based on the histology of these lesions. The fundamental histologic pattern of JNA is composed of vascular channels and connective tissue stroma. They are highly vascular tumours which is reflected by

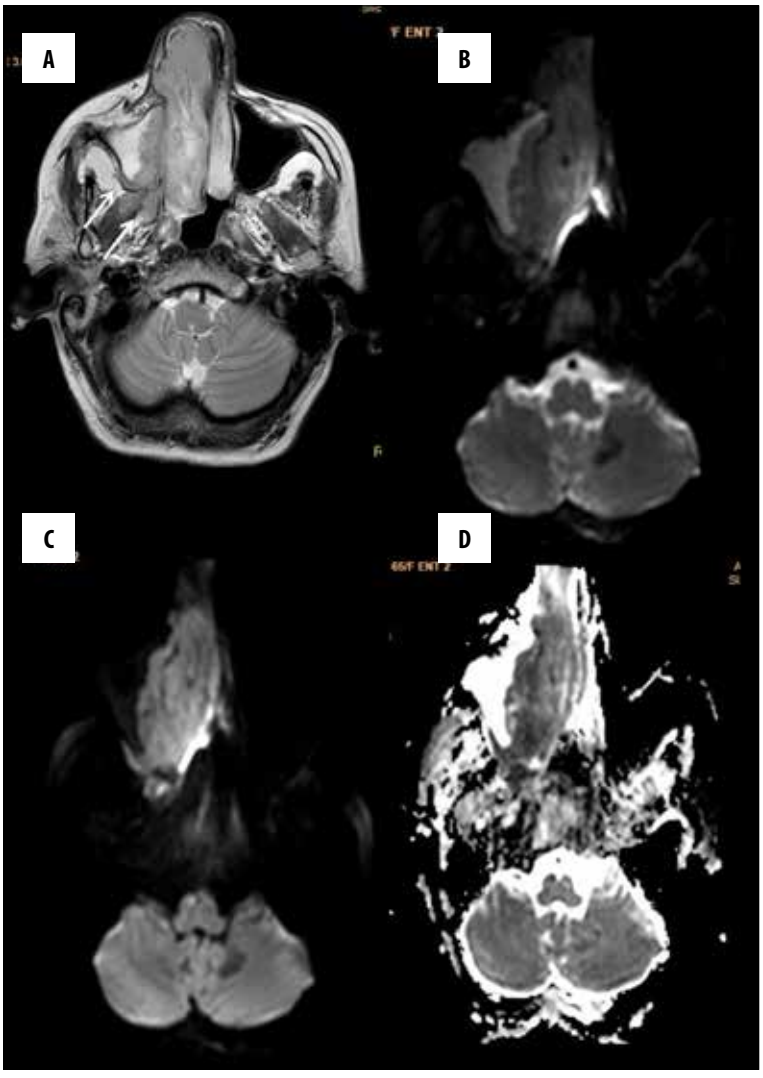

Figure 5. Esthesioneuroblastoma with restricted diffusion. (**A**) Axial T2W image shows a predominantly destructive, right sinonasal mass with erosion of the posterior wall of the right maxillary sinus and involvement of the lateral pterygoid muscle (arrows). DW images at b 0 (**B**), b 1000 (**C**) s/mm^2 and corresponding ADC map (**D**) show restricted diffusion in the mass. Mean ADC value: 0.678×10^{-3} mm^2/s.

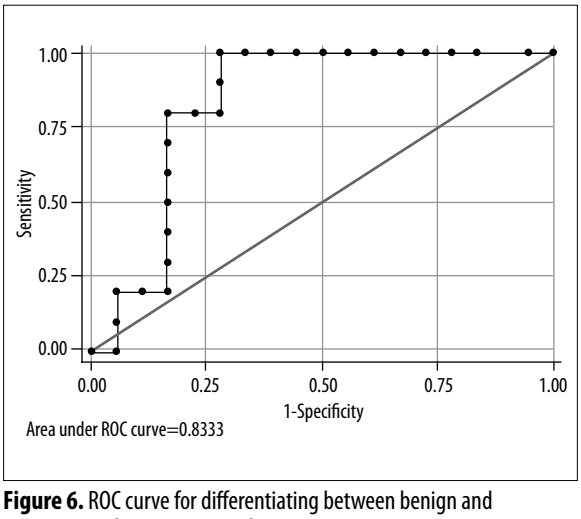

Figure 6. ROC curve for differentiating between benign and malignant sinonasal masses.

a generous distribution of vessels of different calibre in the tumour matrix. The intervening connective tissue stroma is relatively hypocellular and edematous with the presence of plump, spindle-shaped fibroblasts in varying distributions [10]. Owing to the availability of profuse extracellular space, water molecules can have relatively unrestricted movement, thereby leading to facilitated diffusion. In addition to that, their ADC images can have a significant contribution from the high perfusion inherent to these lesions. Although the effect of perfusion predominates at lower b values (<100 s/mm^2), its effect can persist even at higher b values [11,12]. Such distinctly high ADC values seen in JNAs may enable identification of aggressive variants of JNAs, which in spite of being benign may sometimes present with extensive bone destruction and early intra-orbital or intracranial extension, mimicking sinister pathologies such as rhabdomyosarcoma. Since the management plan differs significantly between the two, and biopsy can initiate torrential haemorrhage in JNA, a high ADC value may serve as a useful biomarker for this entity.

The only other entity in our series whose ADC value came close to that of JNAs was a solitary case of sinonasal

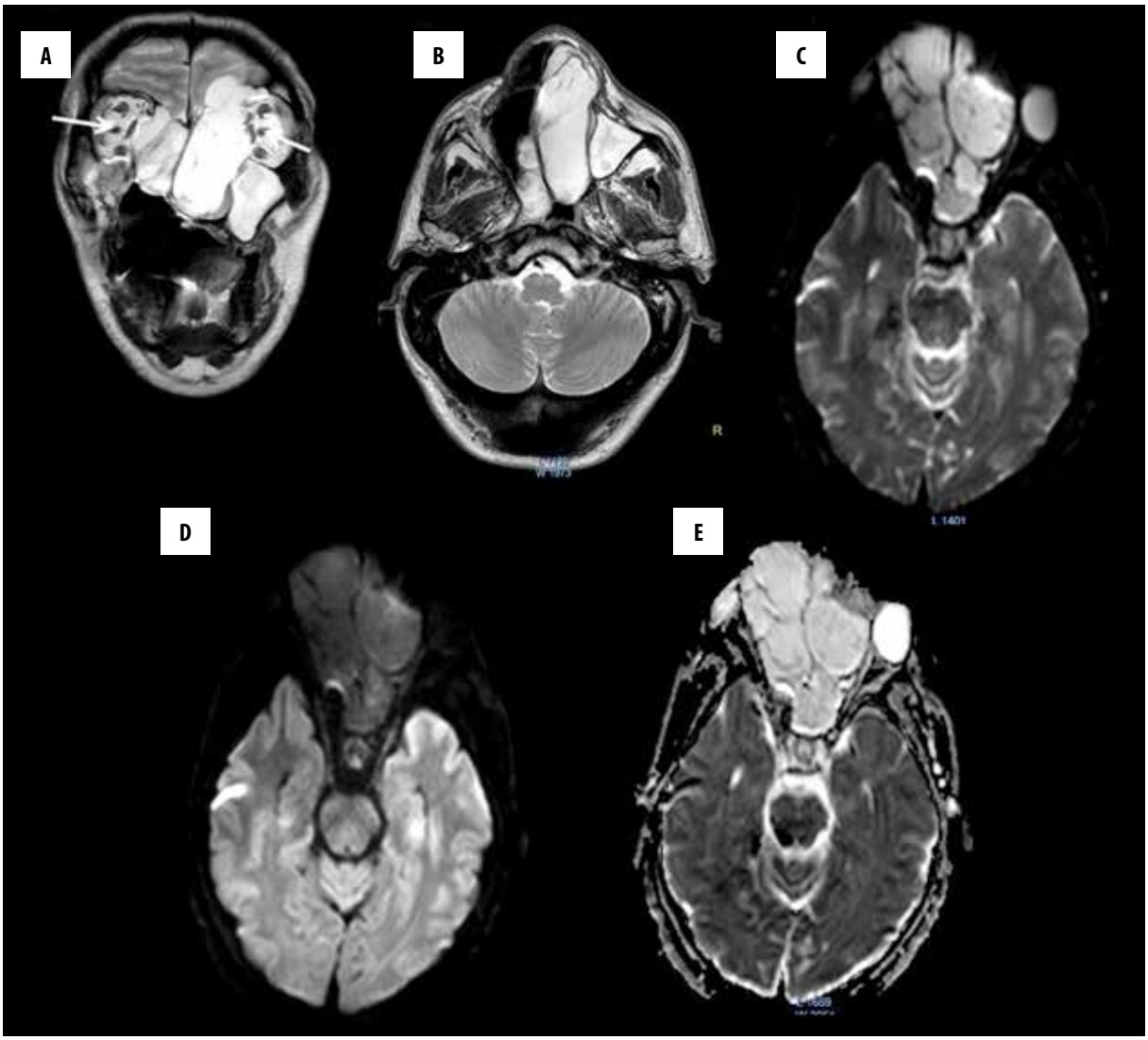

Figure 7. Sinonasal adenocarcinoma: Malignant mass with facilitated diffusion: (**A**) Coronal T2W image shows predominantly expansile, sinonasal mass filling both nasal cavities with extension to both orbits (arrows). Axial T2W image (**B**) shows no extension to pterygopalatine fossa or infratemporal fossa. DW images at b 0 (**C**), b 1000 (**D**) s/mm^2 and corresponding ADC map (**E**) show facilitated diffusion in the mass. Mean ADC value was 2.324×10^{-3} mm^2/s. Biopsy: adenocarcinoma with mucoid material.

adenocarcinoma with abundant mucoid matrix (Figure 7), reiterating the influence of tumour matrix on DW imaging. Similar findings have been reported in mucinous carcinoma of the breast [13] and mucinous carcinoma of the anorectum [14]. This case presented as a predominantly expansile sinonasal mass with intra-cranial and intra-orbital extension. Features typical of JNA such as characteristic widening of the pterygopalatine fossa and/or extension to the infratemporal fossa (Figure 3) were absent in this patient. Hence, DW imaging, when interpreted in conjunction with conventional imaging features, allowed for a confident differentiation of adenocarcinoma from JNA.

Among the benign lesions, only one entity showed restricted diffusion, namely meningioma (Figure 4). Primary extracranial meningiomas in the sinonasal tract usually present as well-defined, enhancing expansile masses with bone remodeling, as was seen in our case [3]. Other authors have used DWI in differentiation between benign and malignant/atypical meningiomas [15,16] and found significantly low ADC values in the latter. Being inherently hypercellular tumours, meningiomas can restrict the movement of water molecules. However, since there was only a single case in our series, no major conclusions can be drawn from our findings.

Of the malignant lesions, esthesioneuroblastoma showed the lowest mean ADC value (Figure 5), possibly explained by its histology which shows small, round malignant cells with scanty cytoplasm with little space for free movement of water molecules [3].

Other malignant entities showing facilitated diffusion were chondrosarcoma, fibromyxoid sarcoma, adenocarcinoma (Figure 7) and adenoid cystic carcinoma (Figure 8). Previous studies have reported facilitated diffusion in

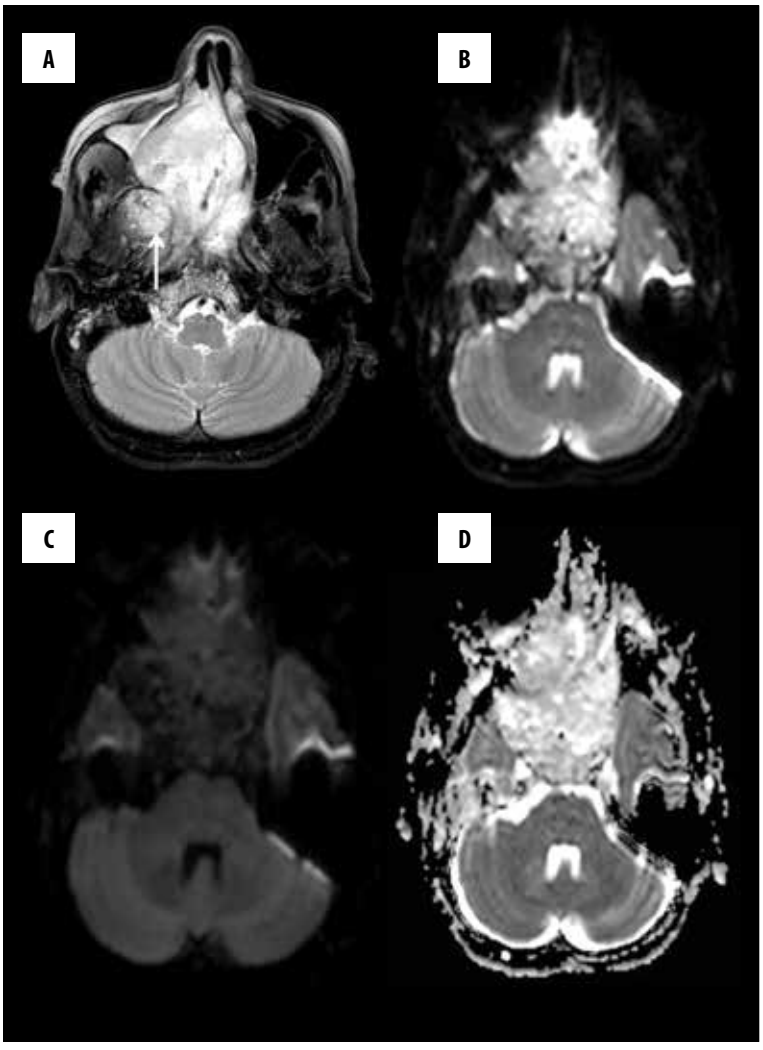

Figure 8. Sinonasal adenoid cystic carcinoma with facilitated diffusion. (**A**) Axial T2W, fat-saturated image shows predominantly expansile right sinonasal mass causing destruction of the posterior wall of the right maxillary sinus and extension to the right infratemporal fossa (arrow). DW images at b 0 (**B**), b 1000 (**C**) s/mm^2 and corresponding ADC map (**D**) show facilitated diffusion in the mass. Mean ADC value: 1.766×10^{-3} mm^2/s.

chondrosarcoma with ADC values reaching as high as $2.051\pm0.261\times10^{-3}$ mm^2/s [17], owing to the sparse cellularity in malignant chondroid matrix [18]. High ADC values have also been reported in myxoid soft tissue sarcoma because of its inherently increased water content [19], explaining similar findings in our solitary case of low grade fibromyxoid sarcoma.

Two cases of sinonasal adenoid cystic carcinoma (Figure 8) also showed facilitated diffusion. Salivary adenoid cystic carcinomas are known to show a speckled pattern of diffusion indicating low to high ADC values [20], which may overlap with those of pleomorphic adenoma [19], as was noted in our study.

There were a few limitations of our study. First, the sample size of our study group was small. Individual entities had inadequate representation in our series, which may have had a significant impact on the results. The spectrum of lesions was heterogeneous in both benign and malignant categories and was, to some extent, influenced by the referral bias of our tertiary care centre. Further studies with larger samples are therefore recommended to validate our findings.

Conclusions

To conclude, DWI has a potential additive role in characterization of sinonasal masses as benign or malignant. While atypical behaviour is shown by entities of both categories, some entities such as JNA show distinctive diffusion characteristics – a finding of immense clinical significance. Unlike benign lesions in other neck spaces, the only benign entity in the sinonasal cavity with restricted diffusion was found to be meningioma. Hence, when used in conjunction with conventional imaging, DWI can further increase the diagnostic confidence of the radiologist.

Statement

This research project received no specific grant from any funding agency in the public, commercial, or not-for-profit sectors

Conflict of interest

Authors declares that there is no conflict of interest.

Table 4. Previous studies using DWI in evaluating sinonasal masses.

S. No	Author	Year	Field strength	No. of patient	b values used (s/mm^2)	Cut-off ADC value ($\times10^{-3}$ mm^2/s)	Benign *vs.* malignant differentiation based on mean ADC value
1	M.L. White et al. [4]	2006	1.5 T	24	0, 1000	NA	Benign: 18.211± 5.2090$\times10^{-4}$ mm^2/s Malignant: 10.752± 4.3987$\times10^{-4}$ mm^2/s Difference: Significant (P<0.0125)
2	A.A. Razek et al. [5]	2009	1.5T	55	0, 500, 1000	1.53 sensitivity: 94% specificity: 92%	Benign: 1.78± 0.41$\times10^{-3}$ mm^2/s Malignant: 1.10± 0.25$\times10^{-3}$ mm^2/s Difference: Significant (P=0.001)
3	M. Sasaki et al. [6]	2011	NA	61	500, 1000	0.84 sensitivity: 61%, specificity: 94%	Benign: 1.35± 0.29$\times10^{-3}$ mm^2/s Malignant: 0.87± 0.32$\times10^{-3}$ mm^2/s Difference: Significant (P<0.0001)
4	M. Sasaki et al. [7]	2011	NA	44	500,1000	NA	Malignant lesions had large (≥50%)areas of low or extremely low ADC values (≤1.2$\times10^{-3}$ mm^2/s)
5	Xin-Yan Wang et al. [8]	2015	3T	197	0, 700, 1000	NA	Benign: WS ADCs# b0, 1000=1.617 $\times10^{-3}$ mm^2/s Malignant: WS ADCs b0, 1000=1.084 $\times10^{-3}$ mm^2/s Difference: Significant (P<0.001)
6	Our study	2013	3T	28	0, 500, 1000	1.791 sensitivity: 80% specificity: 83.3%	Benign: 1.948± 0.459$\times10^{-3}$ mm^2/s Malignant: 1.046± 0.711$\times10^{-3}$ mm^2/s) Difference: Significant (P=0.004)

NA – not available; WS ADC# – whole slice apparent diffusion coefficient.

References:

1. Batsakis J: Tumors of the head and neck: Clinical and pathological considerations. 2nd ed. Baltimore: Williams and Wilkins, 1979; 177–87
2. Madani G, Beale TJ, Lund VJ: Imaging of sinonasal tumors. Semin Ultrasound CT MRI, 2009; 30: 25–38
3. Som PM, Gensler MSB, Kassel EE, Genden EM: Tumors and tumor-like conditions of the sinonasal cavities. In: Som PM, Curtin HD (eds.), Head and neck imaging, 5th ed. St. Louis, Mosby Elsevier, 2011; 253–410
4. White ML, Zhang Y, Robinson RA: Evaluating tumors and tumorlike lesions of the nasal cavity, the paranasal sinuses and the adjacent skull base with diffusion –weighted MRI. J Comput Assist Tomogr, 2006; 30: 490–95
5. Razek AA, Sieza S, Maha B: Assessment of nasal and paranasal sinus masses by diffusion – weighted MR imaging. J Neuroradiol, 2009; 36: 206–11
6. Sasaki M, Eida S, Sumi M, Nakamura T: Apparent diffusion coefficient mapping for sinonasal diseases: Differentiation of benign and malignant lesions. Am J Neuroradiol, 2011; 32: 1100–6
7. Sasaki M, Sumi M, Eida S et al: Multiparametric MR imaging of sinonasal diseases: Time – signal intensity curve- and apparent diffusion coefficient- based differentiation between benign and malignant lesions. Am J Neuroradiol, 2011; 32: 2154–59
8. Wang XY, Yan F, Hao H et al: Improved performance in differentiating benign from malignant sinonasal tumors using diffusion-weighted combined with dynamic contrast-enhanced magnetic resonance imaging. Chin Med J (Engl), 2015; 128: 586–92
9. Srinivasan A, Dvorak R, Perni K et al: Differentiation of benign and malignant pathology in the head and neck using 3T apparent diffusion coefficient values: early experience. Am J Neuroradiol, 2008; 29: 40–44
10. Sternberg SS: Pathology of juvenile nasopharyngeal angiofibroma; A lesion of adolescent males. Cancer, 1954; 7: 15–28
11. Dijkstra H, Baron P, Kappert P et al: Effects of microperfusion in hepatic diffusion weighted imaging. Eur Radiol, 2012; 22: 891–99
12. Padhani AR, Liu G, Koh DM et al: Diffusion-weighted magnetic resonance imaging as a cancer biomarker: Consensus and recommendations. Neoplasia, 2009; 11: 102–25

13. Woodhams R, Kakita S, Hata H et al: Diffusion-weighted imaging of mucinous carcinoma of the breast: evaluation of apparent diffusion coefficient and signal intensity in correlation with histologic findings. Am J Roentgenol, 2009; 193: 260–66
14. Nasu K, Kuroki Y, Minami M: Diffusion-weighted imaging findings of mucinous carcinoma arising in the ano-rectal region: Comparison of apparent diffusion coefficient with that of tubular adenocarcinoma. Jpn J Radiol, 2012; 30: 120–27
15. Filippi CG, Edgar MA, Ulug AM et al: Appearance of meningiomas on diffusion-weighted images: Correlating diffusion constants with histopathologic findings. Am J Neuroradiol, 2001; 22: 65–72
16. Nagar VA, Ye JR, Ng WH et al: Diffusion-weighted MR imaging: Diagnosing atypical or malignant meningiomas and detecting tumor dedifferentiation. Am J Neuroradiol, 2008; 29: 1147–52
17. Yeom KW, Lober RM, Mobley BC et al: Diffusion-weighted MRI: Distinction of skull base chordoma from chondrosarcoma. Am J Neuroradiol, 2013; 34: 1056–61
18. Ginat DT, Mangla R, Yeaney G et al: Diffusion-weighted imaging for differentiating benign from malignant skull lesions and correlating with cell density. Am J Roentgenol, 2012; 198: 597–601
19. Maeda M, Matsumine A, Kato H et al: Soft tissue tumors evaluated by line-scan diffusion-weighted imaging: Influence of myxoid matrix on apparent diffusion coefficient. J Mag Reson Imaging, 2007; 25: 1199–204
20. Eida S, Sumi M, Sakihama N et al: Apparent diffusion coefficient mapping of salivary gland tumors: Prediction of the benignancy and malignancy. Am J Neuroradiol, 2007; 28: 116–21